doi:10.1016/j.jmb.2008.03.034 J. Mol. Biol. (2008) 378, 1064–1073

JMB

Available online at www.sciencedirect.com

ScienceDirect

ELSEVIER

Multiparametric Fluorescence Detection of Early Stages in the Amyloid Protein Aggregation of Pyrene-labeled α-Synuclein

Shyamala Thirunavukkuarasu[1], Elizabeth A. Jares-Erijman[2] and Thomas M. Jovin[1]*

[1]*Laboratory of Cellular Dynamics, Max Planck Institute for Biophysical Chemistry, 37077 Göttingen, Germany*

[2]*Departamento de Química Orgánica, Facultad de Ciencias Exactas y Naturales, Universidad de Buenos Aires, 1428 Buenos Aires, Argentina*

Received 14 December 2007; received in revised form 13 March 2008; accepted 16 March 2008
Available online 26 March 2008

The aggregation of α-synuclein, a presynaptic protein, has an important role in the etiology of Parkinson's disease. Oligomers or protofibrils adopting the cross-β-sheet structure characteristic of fibrillating amyloid proteins are presumed to be the primary cytotoxic species. Current techniques for monitoring the kinetics of α-synuclein aggregation based on fluorescent dyes such as Thioflavin-T and Congo red detect only the terminal fibrillar species, are discontinuous and notoriously irreproducible. We have devised a new fluorescence aggregation assay that is continuous and provides a large set of fluorescence parameters sensitive to the presence of oligomeric intermediates as well as fibrils. The approach involves tagging functionally neutral Ala-to-Cys variants of α-synuclein with the long-lifetime fluorophore pyrene. Upon induction of aggregation at 37 °C, the entire family of steady-state descriptors of pyrene emission (monomer intensity, solvent polarity ratio (I_I/I_{III}), and anisotropy; and excimer intensity) change dramatically, particularly during the early stages in which oligomeric intermediates form and evolve. The pyrene probe senses a progressive decrease in polarity, an increase in molecular mass and close intermolecular association in a manner dependent on position in the sequence and the presence of point mutations. The time-resolved decays (0–160 ns) of intensity and anisotropy exhibited complex, characteristic features. The new assay constitutes a convenient platform for the high-throughput screening of agents useful in the diagnosis and therapy of Parkinson's disease as well as in basic investigations.

Keywords: Parkinson's disease; neurodegenerative; flourescence anisotropy; oligomers; fibrillization

Edited by S. Radford

Introduction

Protein misfolding and anomalous aggregation are features common to many progressive neurodegenerative disorders such as Parkinson's disease (PD) and Alzheimer's disease. In each case, the proteins adopt a cross-β-sheet structure, characteristic of amyloid fibrils and tangles present in the brains of affected individuals.[1,2] The identification, isolation and characterization of oligomeric species arising during amyloid aggregation have acquired great priority due to recent evidence indicating that such "precursors", rather than mature fibrils may be the primary cytotoxic agents leading to neuronal loss.[1,2]

PD is the most prevalent neurodegenerative motor disease of humans, arising from the loss of dopaminergic neurons in the *substantia nigra* of the midbrain.[1] α-Synuclein (AS), a natively unfolded presynaptic protein of 140 amino acid residues,[3] is the principal filamentous component of the Lewy bodies that appear in the brains of patients suffering from PD and other synucleopathies.[1] NMR measurements based on paramagnetic relaxation enhancement and dipolar couplings indicate the existence of an ensemble of conformations of AS, stabilized by long-

*Corresponding author. E-mail address: tjovin@gwdg.de.

Abbreviations used: PD, Parkinson's disease; AS, α-synuclein; ThioT, Thioflavin T.

range tertiary interactions acting to inhibit spontaneous aggregation.[4] The primary sequence is subdivided into three main domains: a N-terminal region (1–60) comprising six imperfect 11 residue KTKEGV repeats and several sites of point mutation (30, 46, and 53) identified in familial PD; a central hydrophobic NAC domain (61–95) serving as the core for aggregation; and a C-terminal domain (96–140) encompassing the numerous acidic residues and prolines.[3] The prefibrillar oligomeric forms of the two AS missense mutations A53T and A30P accumulate more rapidly and persist longer than in the case of wild-type AS, supporting the existence of a direct link between the formation of oligomers and cytopathology.[5]

The aggregation of AS is generally viewed as a mechanism involving nucleation and exponential growth, manifested by an apparent initial lag phase followed by a rapid conversion of the monomeric/oligomeric protein to the terminal fibrillar forms.[1] The kinetics of amyloid formation are monitored *in vitro* by the binding of fluorescent dyes such as Thioflavin T (ThioT) and Congo red,[6] which exhibit a sharp increase in fluorescence intensity upon interaction with the fibrillar structures. However, due to their inherent properties and low concentrations, the intermediate species formed during the lag phase are not detected by the fluorescent probes or by physical methods such as turbidimetry and sedimentation.[6] This circumstance is particularly unfortunate from a biomedical perspective in view of the possibility that the prolonged preclinical phases characteristic of most neurodegenerative diseases may reflect the lag processes observed *in vitro*.[7]

In view of the putative involvement of cytotoxic oligomers, elucidating the molecular events that initiate oligomerization is essential for understanding the underlying pathology and for developing potential therapeutic agents. In this context, access to sensitive methods for the detection of early stages of AS oligomerization is a high-priority objective. Although fluorescence correlation spectroscopy (FCS),[8] electrochemical techniques,[9,10] electron microscopy (EM),[6] and atomic force microscopy.[6,11,12] have proven very useful, the routine application of such techniques for large-scale assays of therapeutically relevant interactions or diagnostic procedures is not feasible. Oligomeric intermediates have been characterized using intrinsic tryptophan fluorescence (Y39W;[13] FRET studies of Y125W/Y133F/Y136F[14]). Yet to the best of our knowledge a continuous assay to monitor the formation of early intermediates during AS aggregation has not been reported.

To achieve both sensitivity and selectivity sufficient for the detection of early aggregates, the very large background signal originating from excess monomeric protein has to be suppressed. We have addressed this issue by the site-specific introduction into the AS molecule of a long-lived and environmentally sensitive fluorescent probe, pyrene. The entire gamut of fluorescence phenomena (intensity, spectral distribution, lifetime, anisotropy) provides a sensitive indicator of all phases of aggregation, particularly the heretofore elusive initial stages that may extend to dimers putatively involved in nucleation.[15] In addition, the pyrene probe distinguishes between wild type and mutant forms and can be adapted to continuous, highly parallelized analytical determinations, such as high-throughput (HTP) drug screening.

Results and Discussion

Monomer suppression: rationale and strategy

N-(1-Pyrene) maleimide was chosen for modification of AS owing to its negligible fluorescence in water and strong emission upon reaction with a cysteine thiol group.[16] Pyrene has ideal properties as a potential probe for monitoring structural and dynamic changes during protein aggregation: a long fluorescent lifetime extending beyond 100 ns under suitable conditions,[17] a relatively high extinction coefficient (36,000 M^{-1} cm^{-1}), excimer formation and solvent-sensitive fluorescence spectra. These diverse fluorescent parameters have been employed widely to assess conformational transitions, polarity[17,18] and probing spatial proximity.[19,20,21] Pyrene has been used to investigate the spatial positioning of the N-terminal and C-terminal segments of AS bound to a membrane,[22] but not for monitoring aggregation.

Despite the diverse applications of the unique spectroscopic properties of pyrene, reports based on fluorescence anisotropy have been relatively few. The appropriate range of recoverable rotational correlation times (ϕ) for a fluorophore with a fluorescence lifetime (τ), is dictated by the relationship $0.1 < \sigma = \tau/\phi < 10$.[23] Free pyrene exhibits low steady-state fluorescence anisotropy as a consequence of its long fluorescence lifetime, which in many cases exceeds the rotational correlation times of the macromolecules to which it is conjugated. This circumstance applies in particular to monomeric AS, which exhibits an apparent ϕ of 1–2 ns (Ref. 24, this study and Bertoncini, C. W. *et al.*, unpublished data). Thus, in the case of protein aggregation, one would anticipate a pronounced increase in the anisotropy of conjugated pyrene within the temporal window dictated by its inherently long fluorescence lifetime, particularly if the latter increases (as observed) due to polarity effects. These expectations were realized in the present study, in which significant changes in fluorescence anisotropy were detected immediately after the initiation of aggregation of a mixture of pyrene-labeled AS and unlabeled protein.

The primary sequence of wild-type AS lacks cysteine, necessitating the introduction of Ala-to-Cys mutations to provide sites for labeling. Our studies were carried out with three variants of the wild-type AS with cysteine replacements at positions 18, 90, and 140 (A18C, A90C and A140C; Fig. 1a). The introduction of pyrene by reaction with these residues did not significantly alter the UV CD spectrum (see Supplementary Data, Fig. 1). The peak in the vacuum UV region of 190–205 nm characteristic of the unstructured monomer protein was retained and we

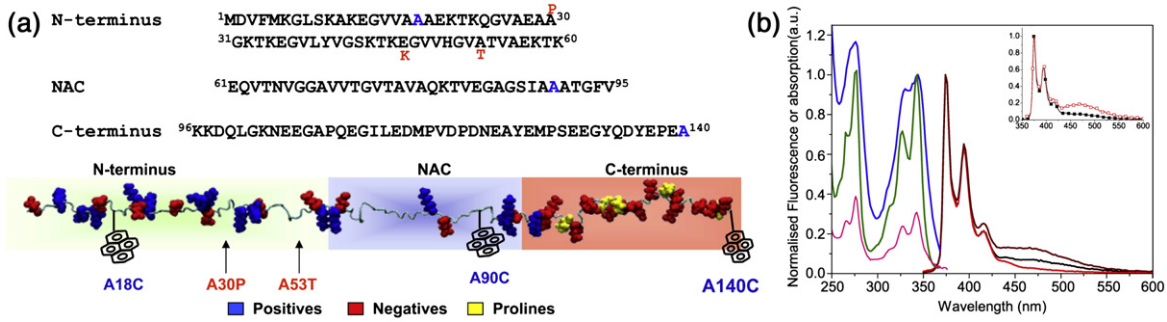

Fig. 1. (a) Primary sequence of AS. The disease-related familial mutations are in red (A30P, A53T, and E46K) and the cysteine variants are in blue. Below, the sequence of AS as a polypeptide backbone indicating the points of attachment of the pyrene fluorophore. (b) Absorption, fluorescence excitation and emission spectra of pyrene-labeled wild-type AS cysteine variants. Normalized (at 343 nm) excitation (emission at 375 (▬) or 465 (▬) nm) and absorption spectra (▬) for AS-A90C_Py. Emission spectra for AS-A18C_Py (▬), AS-A90C_Py (▬), and AS-A140C_Py (▬) normalized at 375 nm. The inset shows the normalized emission spectra of AS-A90C_Py, with excitation at 340 nm (■) and 352 nm (□). Protein, 17 μM; pyrene, 6 μM in buffer 25 mM sodium phosphate, pH 6.2.

attribute the slight changes in ellipticity to contributions from the pyrene moiety.[25]

Fluorescence properties of pyrene-labeled AS

The fluorescence emission spectra of all the pyrene-labeled cysteine variants displayed three well-defined pyrene monomeric peaks in the near-UV at 375 nm, 395 nm and 415 nm (Fig. 1b).[18] An additional low-intensity broad shoulder at 465 nm was present in the case of AS-A90C_Py and AS-A18C_Py, attributable to an excimer band that characteristically lies in the region of 450–475 nm. The excimer is a dimer of an excited state pyrene and a second molecule in the ground state.[26] Its formation requires close proximity (<5 Å) achieved either by judicious intramolecular placement of two probes or via translational diffusion and intermolecular collisional encounter of single-labeled proteins at concentrations of >10–100 μM.[27]

The excitation peaks of the excimer were broader, and the two shoulders at 266 nm and 312 nm were less distinct than in the case of the monomer. Similar data for other pyrene–protein adducts have been reported.[20] The excimer fluorescence also increased with red-edge excitation (Fig. 1b, inset) and was reduced by addition of excess unlabeled protein in the case of the label at position 18 but not at position 90. These properties suggest that the excimer fluorescence originated from a distinct yet low-abundance sub-population of pyrene-labeled molecules, e.g. AS dimers such as those postulated to act as nucleation centers.[15] In the case of AS-A90C_Py, the excimer is apparently stabilized by ground state pyrene–pyrene contacts acting synergistically with the hydrophobic NAC region at the intermolecular interface, and thereby fulfills the definition of a "static excimer".[26] The very low excimer level of AS-A140C_Py can be attributed to the extended conformation adopted by the highly negatively charged C terminus,[3] (Fig. 1a), which remains unstructured even in fibrillar states.[28]

Aggregation kinetics of pyrene-labeled AS monitored by pyrene fluorescence

The aggregation of pyrene-labeled AS preparations was generally followed in three or more replicates by measuring the steady-state fluorescence intensity and fluorescence anisotropy of the pyrene probe, in parallel with ThioT fluorescence of aliquots removed periodically from the incubations. Pyrene-labeled wild-type and mutant AS added in trace amounts (pyrene to protein ratio of 1:16) to solutions of the corresponding unlabeled protein aggregated at the same rate as the latter, according to the ThioT assays (Supplementary Data, Fig. 2).

The fluorescence spectra of AS-A18C_Py, AS-A90C_Py, AS-A140C_Py, and the two mutants AS-A30P-A90C_Py and AS-A53T-A90C_Py changed dramatically and exhibited distinctive profiles during the course of aggregation (Fig. 2). The fluorescence intensity at the four vibrational maxima of pyrene (375 nm, 383 nm, 395 nm, and 405 nm), and the excimer emission at 465 nm are shown in Fig. 3. The pyrene monomer bands of AS-A18C_Py and AS-A140C_Py increased by >100% during the first 36 h and continued to increase, corresponding to the rise in ThioT signal denoting the fibrillization of the bulk protein. We attribute the appearance of distinct emission peak at 385 nm (Fig. 2) to a local increase in the hydrophobicity of the protein rather than aminolysis,[20] since protein labeling and aggregation were performed at low pH (6.2). The third positional variant of wild-type AS, AS-A90C_Py, displayed a different spectral profile during aggregation (Fig. 2b), featuring a large increase, not observed with AS-A18C_Py, of the pre-existent excimer peak and an accompanying quenching of the monomer (clearly seen in the 28 h data). After fibrillization, the 385 nm peak had the highest intensity.

The final intensity of the excimer signal increased dramatically with the fractional concentration of the pyrene-labeled protein in the aggregation mixture (Fig. 2b, inset; Supplementary Data Fig. 3). The cor-

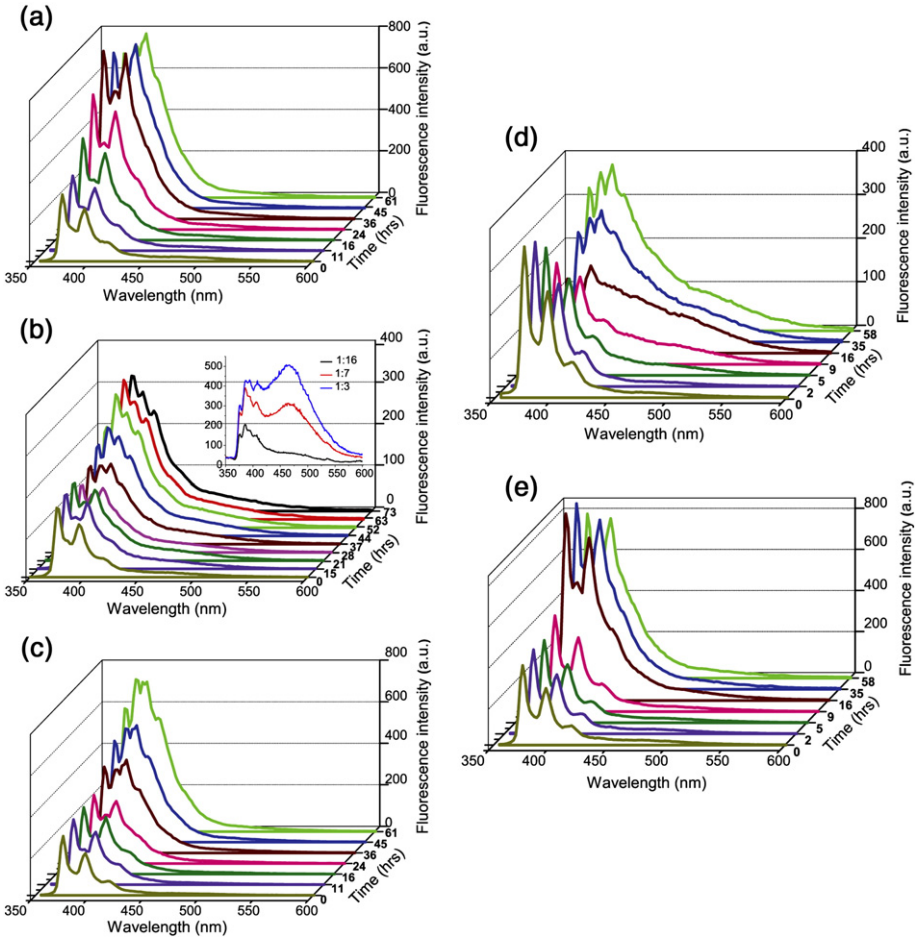

Fig. 2. Emission spectra of pyrene-labeled AS cysteine variants after incubation at 37 °C for different lengths of time. (a) AS-A18C_Py; (b) AS-A90C_Py; (c) AS-A140C_Py; (d) AS-A30P-A90C_Py; (e) AS-A53T-A90C_Py.The pyrene-labeled protein was diluted 16-fold with the corresponding unlabeled protein (wild-type AS for the three wild-type cysteine variants; AS-A30P for the AS-A30P-A90C, and AS-A53T for AS-A53T-A90C). The fluorescence spectra correspond to one of the replicates. Protein, 100 μM; pyrene, 6 μM. The inset in b shows the excimer fluorescence intensity at different dye–protein ratios at the end of aggregation.

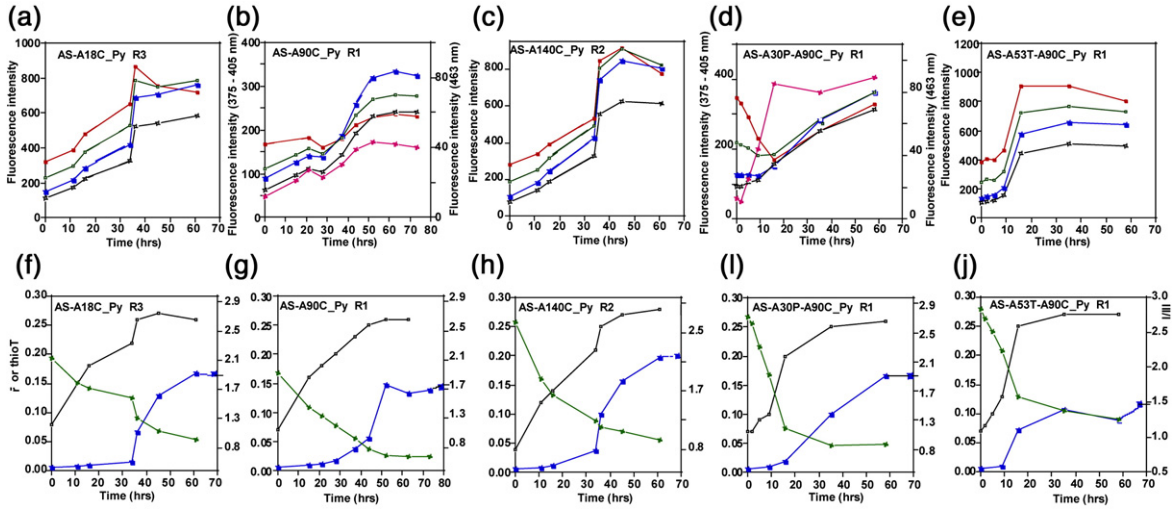

Fig. 3. Spectral parameters of all the positional pyrene variants of AS monitored during aggregation. (a–e) Fluorescence intensity at the four vibrational peaks 375 nm (—), 385 nm (—), 393 nm (—), 405 nm (—), 463 nm (—). (f–j) Fluorescence anisotropy (—), I_I/I_{III} ratio (—) and un-normalized ThioT fluorescence (—), for one of the replicates. The molecules are identified in each panel.

responding ThioT and anisotropy curves for the different fractional concentration of pyrene are given in Supplementary Data Fig. 4. For the pyrene-total protein ratios, α, of 1:16, 1:7, and 1:3 the relative excimer intensity after completion of aggregation was 1:4:8. Thus, the excimer signal constitutes a very sensitive indicator of association, reflecting stacking interactions of pyrene promoted by the tertiary and quaternary structural features of both oligomeric and fibrillar forms of AS. During aggregation, AS adopts the cross-β-conformation characteristic of all amyloid fibrils, but the relative orientation of the constituent protein monomers is a matter of controversy.[29–31] Assuming that a pyrene at position 90 of the AS core (NAC) in a fibrillar substructure can potentially engage in excimer-forming interactions with neighbors above, below, and opposite,[28] the relative probability of encountering a second pyrene in one of the available loci would be approximately proportional to α, with relative excimer yield estimates of 1:2:5, values in reasonable agreement with the experimental findings. Thus, the excimer data point to an "in-register" orientation of the β-sheets in the core region. The documented unfolded and disordered states of the N and C termini in fibrillar bundles[28] would not favor the encounter of two pyrene molecules to form excimers, accounting for the absence of increase in excimer intensity upon aggregation of AS.

The two familial AS mutants A53T-A90C_Py and A30P-A90C_Py, although labeled at the identical position, showed strikingly different spectral signatures (Figs. 2 and 3). As expected, the ThioT signals from these aggregation-prone mutants of AS increased earlier in the incubation, albeit more gradually in the case of A30P-A90C. The pyrene monomer intensities, including the 385 nm component, increased as before with AS-A53T-A90C_Py but decreased with AS-A30P-A90C_Py due to the development of the enhanced excimer signal at the cost of the monomer. In contrast, only very low excimer fluorescence appeared during the final stages of aggregation of AS-A53T-A90C_Py. Apart from the difference in their rates of aggregation, these two PD variants also differ with respect to lipid binding, toxicity in yeast-based assays,[32] and protofibrillar structure.[33] The small excimer signal exhibited by A53T-A90C_Py denotes the existence of distinctive conformational features preventing intermolecular pyrene–pyrene interactions, whereas the opposite holds for A30P-A90C_Py. Solid-state NMR studies are being conducted by the group of M. Baldus to elucidate the distinctive structural features at the fibrillar level responsible for these phenomena.

In comparative aggregation assays with mixtures of A30P-A90C_Py and unlabeled genetic mutant A30P or wild-type AS, the pyrene-labeled "mutant" mirrored the aggregation kinetics of the bulk protein (Supplementary Data Fig. 5). In addition, the pyrene exhibited the spectral properties corresponding to the "majority" protein. Thus, pyrene-based aggregation assays reveal a previously undetected capability of AS for "molecular adaptation" to the structural framework dictated by other co-aggregating molecules present in excess. This principle may well apply to the heterogeneous molecular associations characteristic of the aggregopathy diseases in general.[1,2]

The pyrene I_I/I_{III} ratio: a sensitive indicator of early oligomers

The relative changes in intensity of the characteristic vibronic bands of pyrene monomer fluorescence reflect the changing polarity of the microenvironment. The ratio of the intensities of the third (385 nm) and first (375 nm) bands, I_I/I_{III} forms the basis of the *Py* scale of polarity.[18] A lower I_I/I_{III} band ratio corresponds to a non-polar environment (cyclohexane: 0.58) whereas a higher value indicates greater polarity (DMSO: 1.95). The initially high I_I/I_{III} value of pyrene, conjugated to AS (Fig. 3f–j) was close to that observed in methanol, a result consistent with the low overall hydrophobicity of natively unfolded proteins.[34] A significant and continuous drop in I_I/I_{III} ratio during the pre-fibrillar phase of aggregation, in the case of all the labeled AS variants (Fig. 3f–j), attested to a gradual increase in the local hydrophobicity of the protein, presumably due to the progression of small oligomeric precursors to higher-order proto-fibrillar filamentous intermediates of AS.

Steady-state fluorescence anisotropy of pyrene-labeled AS

In the case of an isotropic rotator undergoing hindered (anisotropic) motion, the steady-state anisotropy is related to the fluorescence lifetime normalized by the rotational correlation time, according to the expression $r=(r_o+r_\infty\sigma)/(1+\sigma)$, where r_o and r_∞ are the fundamental (initial) and limiting (terminal) anisotropies, respectively, dictated by the orientations of the absorption and emission transition moments of the fluorophore relative to themselves and to the molecular frame before and after rotation. For molecules isotropically distributed in solution, $0.4>r>-0.2$. The great sensitivity of fluorescence anisotropy in the context of the system reported here derives from the dual circumstance alluded to earlier: the operational suppression of the monomer contribution and the influence of varying σ ratios during oligomerization.

All pyrene-labeled AS variants demonstrated a very large rise in the steady-state anisotropy measured at the monomer emission band from an initial value <0.1 to a final level of >0.25 (Fig. 3f–j). The time-course paralleled the decrease in I_I/I_{III} values and preceded the rise in ThioT signals. The final *r* of 0.25–0.27 was close to the intrinsic r_o of pyrene; i.e. for the immobilized probe ($r_o=0.3$ in 3-methylpentane glass at 77 K).[35]

The fluorescence anisotropy of a labeled protein at any given time is an intensity-weighted average of the individual values of the various species present in the molecular population. In the case of aggregating AS: (i) monomer, oligomers, protofibrils during the lag phase (ThioT negative); and (ii) fibrils present

during the final stages of aggregation (ThioT positive) coexisting with the species cited under (i). The fluorescence anisotropy achieved its maximal value at the time-point corresponding approximately to the $t_{1/2}$ of the ThioT signal. ThioT interacts specifically with the cross-β-sheet structure common to amyloid fibrils, and the binding is independent of the primary structure of the protein.[36] Only the multimeric fibrillar forms give rise to a significant fluorescence emission upon binding of the dye. Thus, we attribute the changes in fluorescence intensity and fluorescence anisotropy of pyrene during the lag phase defined by the ThioT progress curve to the formation of "protofibrillar" oligomeric species, spheroids, chains of spheres etc. as revealed by atomic force microscopy.[11,37] This determination obliges us to consider intermediate kinetic steps of oligomerization in the nucleation-propagation model, involving molecular species differing in important respects from the ultimate fibrillar form. Details of such a model will be presented elsewhere.

A semi-quantitative comparison of the changes in the steady-state spectroscopic signature of labeled pyrene in the wild-type and mutant forms of AS are summarized in Supplementary Data Table 1. All the photophysical parameters of labeled pyrene (fluorescence intensity, solvent polarity ratio I_I/I_{III}, excimer formation, and anisotropy), provide a convenient means for monitoring AS oligomerization and fibrillization *in vitro* in the very early stages.

Fluorescence lifetime of pyrene-labeled AS

Time-resolved fluorescence anisotropy has been used to monitor the aggregation of a commercially available Aβ 1–40 fluoropeptide bearing a fluorescein tag.[38] However, the short excited state lifetime of fluorescein (3–4 ns) precludes the quantification of aggregates undergoing rotational depolarization on a timescale much longer than that of the probe itself. The utility of long-lived fluorescent probes such as pyrene was already manifested in the steady-state measurements discussed above, but mechanistic studies of the kinetics and pathways of oligomerization as well as the implementation of new assay/diagnostic procedures required recourse to time-resolved determinations.

The fluorescence lifetime of all the pyrene-labeled AS preparations at room temperature exhibited triexponential decays typical for this fluorophore,[20] with a short-lived component of 2–10 ns, an intermediate component of 10–35 ns, and a long-lived component of 45–120 ns (Fig. 4). The three fluorescence lifetimes doubled, and their respective fractional contributions varied, during all phases of aggregation, indicating systematic changes in the microenvironment(s) of the pyrene probe. A53T-A90C_Py, was the notable exception, with lifetime values that were high from the onset (>100 ns) and remained fairly constant. The finding that the fractional contribution of the shortest lifetime was greater for the end-labeled molecules and decreased during aggregation was not unexpected. In contrast, the intermediate lifetime of the A90C_Py variants made the highest initial contribution, which then decreased during the aggregation, probably due to competition from the excimer. As a consequence, the longest component increased in amplitude.

The multi-exponential decay of single-site pyrene-labeled AS molecules may reflect the different modes of association of the pyrene ring with the protein surface; i.e. with the bulk of the ring buried and the succinimide moiety exposed to water or vice versa.[39] It is equally, or more, probable that the complex temporal pattern reflected in the lifetime (and anisotropy, see below) data reflects the different, coexist-

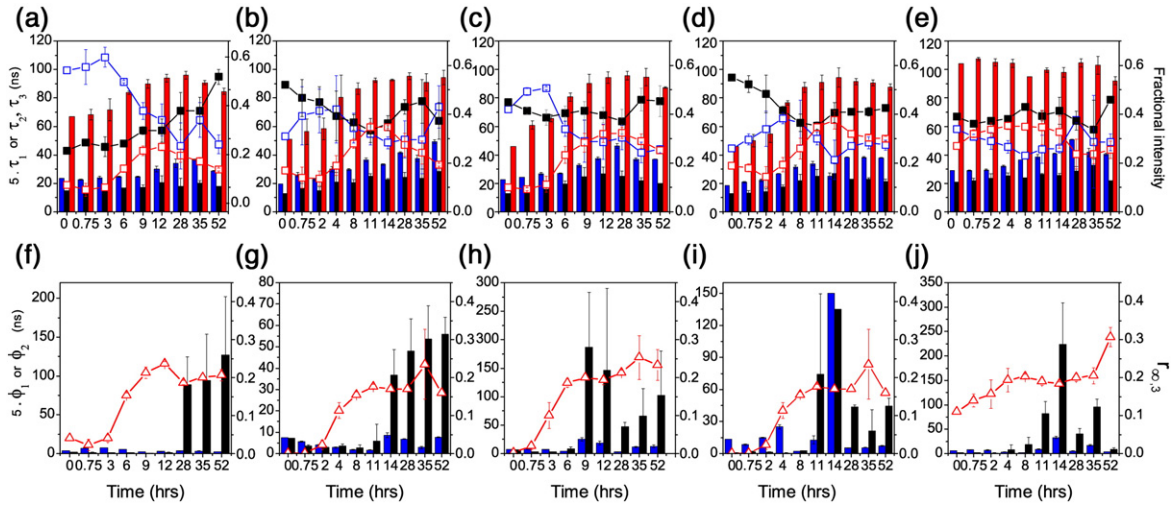

Fig. 4. Time-course of fluorescence intensity and anisotropy decay parameters during aggregation of pyrene-labeled AS. (a and f) AS-A18C_Py. (b and g) AS-A90C_Py. (c and h) AS-A140C_Py. (d and i) AS-A30P-A90C_Py. (e and j) AS-A53T-A90C_Py. Top panel: Fluorescence lifetimes (bars, left-hand axis) and corresponding fractional intensities (right-hand axis). τ_1, f_1 (blue), τ_2, f_2 (black), τ_3, f_3 (red). Bottom panel: Rotational correlation times (bars, left-hand axis). ϕ_1 (blue), ϕ_2 (black). Residual anisotropy (right-hand axis), $r_{\infty,3}$ (Δ). The indicated error bar is the standard deviation.

ing, and evolving protein species and environments detectable by the pyrene probe. The fluorescence lifetimes of pyrene monitored via the excimer emission band (2.8 ns, 13 ns, 48 ns, for AS-A90C_Py) were in the same range as the monomer components. The fluorescence of pyrene, either free or as a covalent protein adduct, is subject to collisional quenching by molecular oxygen. Pyrene exhibits a single long fluorescence lifetime of ~300 ns in benzene in the absence of oxygen.[17] Oxygen-scrubbed (using glucose oxidase) solutions of AS-A90C_Py showed an increase in the steady-state excimer and a decrease in the monomer emissions. The fluorescence lifetimes of the monomer and excimer also increased from 45 ns to 73 ns, and from 48 ns to 53 ns, respectively. The measurements otherwise reported in this study were performed in oxygen-saturated solutions.

Comparable hydrostatic pressures are required for dissociation of oligomeric proteins and amyloid fibrils, suggesting the existence of packing defects and hydrophobic pockets in the latter.[40] These structural elements constitute the targets for hydrophobic compounds such as *N*-arylaminonaphthalenesulfonates[24] but are apparently also sensed by the pyrene probes attached to the protein backbone, as manifested by the trends in fluorescence lifetimes during the course of aggregation. The observation that the fluorescence lifetimes of the pyrene-labeled PD variant AS-A53T were long and relatively invariant during aggregation, and that this mutant is more susceptible to pressure-induced disruption[40] point to possible differences in fibrillar architecture of the wild-type and genetic AS mutants. Solid state NMR studies by H. Heise and M. Baldus on fibrils of wild-type AS and the genetic AS mutant A53T reveal differences in the core domain (unpublished results).

Time-resolved fluorescence anisotropy: "rising" anisotropy curves

The concerted decays of fluorescence intensity and anisotropy of a pyrene-labeled protein during the aggregation were measured and interpreted according to an associated exponential model in which the fluorescence lifetime and amplitude of the total intensity decay components are linked specifically with individual anisotropy parameters.

$$r(t) = \sum_{i=1}^{n} f_i(t) r_i(t) \tag{1}$$

where:

$$f_i(t) = \frac{\alpha_i e^{-t/\tau_i}}{I_T(t)}, I_T(t) = \sum_{i=1}^{n} \alpha_i e^{-t/\tau_i} \tag{2}$$

and:

$$r_i(t) = (r_{o,i} - r_{\infty,i}) e^{-t/\phi_i} + r_{\infty,i} \tag{3}$$

The latter expression represents the simplest possible representation of the hindered rotational relaxation alluded to above; ϕ_i is the *i*th apparent rotational correlation time, $r_i(t)$, α_i and τ_i are the *i*th fluorescence amplitude and lifetime, and $r_{o,i}$ is the initial pre-rotational anisotropy. The time-resolved anisotropy was fit with Kaleidagraph (v3.5, Synergy Software) to a function in which each rotational component was weighted by its respective intensity function (Eq. (1)), the parameters of which were obtained from the analysis of the associated intensity decay data. We assumed (and confirmed in most cases) that the AS monomer, present at the start of incubation, underwent a virtually isotropic decay, i.e. with $r_\infty = 0$.

In most cases, the three resolved fluorescence lifetimes were fit successfully to two rotational correlation times ϕ, and a third infinite component corresponding to an immobile species (over the time-course of the measurement). In the case of AS-A30P-A90C_Py, three finite rotational correlation times were required at the start of incubation to obtain an adequate fit. The rotational correlation times and the values of $r_{\infty,3}$ during the aggregation assay are shown in Fig. 4f–j.

At the beginning of aggregation, the fluorescence anisotropy of the pyrene-labeled proteins, with the exception of A53T-A90C_Py, decayed to values close to zero (0.002) with two rotational correlation times of the order 1 ns to 5 ns. From 45 min to 3 h after the start of incubation, the limiting anisotropy, $r_{\infty,3}$ increased significantly (0.02) and thereafter rose to values in the range of 0.2 ± 0.05. The complex interplay between the decay of intensity and rotational motion resulted in the time-dependent anisotropy (AS-A90C_Py) shown in Fig. 5. Such unusual bimodal anisotropy "decay" curves clearly reflect a heterogeneous environment, with a long-lifetime component coupled to a long (or virtually "infinite") rotational correlation time. The observed trend in the anisotropy decay curves arise as a result of multiple species with different parameters. (Rising anisotropy curves are observed when the major contribution to the fluorescence decay is from the fast component and the ratio of the long to short lifetimes is >3.[41])

The behavior of time-resolved anisotropy can be interpreted in terms of the various AS molecular species as follows. The anisotropy decay at time zero represents the AS monomer, whereas the major contribution to the anisotropy decay with high residual anisotropy observed at the end of aggregation derives from AS fibrils. The anisotropy curves observed at the intermediate time-points of aggregation reflect the contribution of monomeric and oligomeric AS. The initial stages of aggregation, i.e. the ThioT-negative phase, are witnessed by an increase in the residual anisotropy with the time-resolved anisotropy decay showing an upward signature and two rotational correlation times of 1–5 ns. During this phase, the rotational correlation time associated with the intermediate lifetime component either equals or is greater to that associated with fast decay component (Fig. 4g). The rising anisotropy curves report the formation of oligomers with a rotational correlation time greater than that of the monomer.

As the aggregation proceeds, the magnitude of the upward trend in anisotropy increases as the oligo-

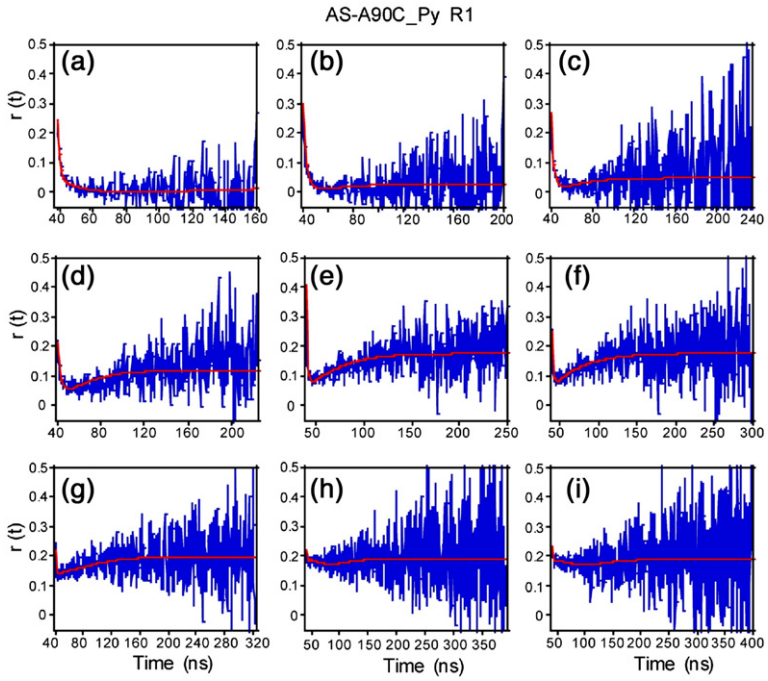

Fig. 5. Time-course of anisotropy decay for AS-A90C_Py at different time-points during the aggregation. Red lines, fitted data according to Eq. (1). Time (h) and $r_{\infty,3}$ values; (a) 0 h, 0.002; (b) 45 min, 0.03; (c) 2 h, 0.05; (d) 4 h, 0.12; (e) 8 h, 0.17; (f) 11 h, 0.18; (g) 14 h, 0.20; (h) 35 h, 0.19; (i) 52 h, 0.19.

mers grow in number and size, reflected in a progressively increasing $r_{\infty,3}$. The leveling out of residual anisotropy close to the limiting anisotropy value of pyrene[35] occurs when the ThioT signal reaches half its maximal value. The incorporation of oligomers and other higher aggregates into protofibrils or fibrillar material results in an increase in the correlation time associated with the long lifetime component to almost ten times its initial value (~60 ns for AS-A90C_Py). The fibrils themselves are virtually immobile during such measurements; the short rotational correlation times recovered even during the final stages of aggregation are presumably due to the residual fraction of monomeric AS. In general the longest resolved rotational correlation time recovered for all the pyrene-labeled protein was in the range of 60–150 ns, with the exception of AS-A53T-A90C_Py, for which the rotational correlations times were as long as 250 ns at the end of the reaction.

An exception to the course of anisotropy in the pyrene-labeled AS variants was provided by A53T-A90C, which exhibited an upward curvature right from the start of incubation (Supplementary Data Fig. 6). It is noteworthy that this genetic mutant of AS also differed from the other molecules by virtue of exhibiting a long fluorescence lifetime that remained virtually unaltered throughout the aggregation assay. However, the high residual anisotropy of AS-A53T-A90C_Py could have reflected the existence of small preformed nucleation sites or incipient aggregates of appreciable size and rigidity. Such molecular species would have to have persisted after the step of ultracentrifugation preceding the incubation and/or to have formed spontaneously through fairly rapid equilibration.

During the completion of this manuscript, a fluorescence polarization assay for rapid screening of AS oligomerization/fibrillization inhibitors was reported.[42] The measurements were based on random labeling with short lifetime fluorophores and thus lacked the selectivity and sensitivity afforded by both the steady-state and time-resolved intensity and anisotropy signals reported here, both of which offer great potential for high throughput screening (HTS) in drug discovery. The pyrene-based assay reveals important molecular changes during aggregation via an array of fluorescence parameters, shedding light on the key roles of molecular segments such as the N and the C termini, and the core NAC region during early, middle, and late phases of AS aggregation. This feature is of particular importance in view of the fact that potential therapeutic PD drugs are generally screened for their ability to inhibit fibril formation, without addressing their effects on critical prefibrillar intermediates.[37] We also anticipate the application of pyrene conjugates of AS to study aggregation *in vivo* (cellular systems) by monitoring the pyrene monomer anisotropy and excimer fluorescence.

Methods

Protein expression, purification, and labeling

Recombinant human wild-type and the genetic (A53T and A30P) mutants of AS were expressed and purified as described.[11] The cysteine variants of AS (A18C, A90C, A140C, A53T-A90C, and A30P-A90C) were constructed using the Quick-Change site-directed mutagenesis kit (Stratagene), and the introduced modifications were verified by DNA sequencing.

Labeling of AS with *N*-(1-pyrene) maleimide

The protein preparations were labeled with *N*-(1-pyrene) maleimide (Molecular Probes, Invitrogen) as

suggested by Molecular Probes (Supplementary Data) in 25 mM sodium phosphate, pH 6.2. The labeling efficiency (70–85%) was calculated using a molar extinction coefficient of 36,000 M^{-1} cm^{-1} at 343 nm for pyrene.[43] For details refer to Supplementary Data.

Steady-state and time-resolved spectroscopic measurements

The corrected excitation and emission spectra of pyrene labeled AS variants were measured on a Cary Eclipse spectrofluorimeter with slit-widths of 5/5 nm. Time-resolved fluorescence and anisotropy was recorded in the forward mode using an IBH 5000 U fluorescence lifetime spectrometer equipped with LED light sources and a TBX-04-A detector. More detailed description of these and other procedures can be found in the Supplementary Data.

Acknowledgements

We thank Drs C W Bertonicini, R Rasia, M S Celej, V Subramaniam, H. Heise and M. Baldus for valuable suggestions and discussions, and providing data before publication, and G Heim for technical assistance. S.T. is a recipient of a postdoctoral fellowship from the Max Planck Society (Toxic Protein Conformation Project).

Supplementary Data

Supplementary data associated with this article can be found, in the online version, at doi:10.1016/j.jmb.2008.03.034

References

1. Chiti, F. & Dobson, C. M. (2006). Protein misfolding, functional amyloid, and human disease. *Annu. Rev. Biochem.* **75**, 333–366.
2. Hamley, I. W. (2007). Peptide fibrillization. *Angew Chem. Int. Ed. Engl.* **46**, 8128–8147.
3. Hoyer, W., Cherny, D., Subramaniam, V. & Jovin, T. M. (2004). Impact of the acidic C-terminal region comprising amino acids 109–140 on α-synuclein aggregation in vitro. *Biochemistry*, **43**, 16233–16242.
4. Bertoncini, C. W., Jung, Y. S., Fernandez, C. O., Hoyer, W., Griesinger, C., Jovin, T. M. & Zweckstetter, M. (2005). Release of long-range tertiary interactions potentiates aggregation of natively unstructured α-synuclein. *Proc. Natl Acad. Sci. USA*, **102**, 1430–1435.
5. Rochet, J. C., Conway, K. A. & Lansbury, P. T., Jr. (2000). Inhibition of fibrillization and accumulation of prefibrillar oligomers in mixtures of human and mouse α-synuclein. *Biochemistry*, **39**, 10619–10626.
6. Harper, J. D. & Lansbury, P. T., Jr (1997). Models of amyloid seeding in Alzheimer's disease and scrapie: mechanistic truths and physiological consequences of the time-dependent solubility of amyloid proteins. *Annu. Rev. Biochem.* **66**, 385–407.
7. Selkoe, D. J. (2003). Folding proteins in fatal ways. *Nature*, **426**, 900–904.
8. Giese, A., Bader, B., Bieschke, J., Schaffar, G., Odoy, S., Kahle, P. J. *et al.* (2005). Single particle detection and characterization of synuclein co-aggregation. *Biochem. Biophys. Res. Commun.* **333**, 1202–1210.
9. Masařík, M., Stobiecka, A., Kizek, R., Jelen, F., Pechan, Z., Hoyer, W. *et al.* (2004). Sensitive electrochemical detection of native and aggregated α-synuclein protein involved in Parkinson's disease. *Electroanalysis*, **16**, 1172–1181.
10. Paleček, E., Ostatná, V., Masařík, M., Bertoncini, C. W. & Jovin, T. M. (2008). Changes in interfacial properties of α-synuclein preceding its aggregation. *Analyst*, **133**, 76–84.
11. Hoyer, W., Antony, T., Cherny, D., Heim, G., Jovin, T. M. & Subramaniam, V. (2002). Dependence of α-synuclein aggregate morphology on solution conditions. *J. Mol. Biol.* **322**, 383–393.
12. van Raaij, M. E., Segers-Nolten, I. M. & Subramaniam, V. (2006). Quantitative morphological analysis reveals ultrastructural diversity of amyloid fibrils from α-synuclein mutants. *Biophys. J.* **91**, L96–L98.
13. Dusa, A., Kaylor, J., Edridge, S., Bodner, N., Hong, D. P. & Fink, A. L. (2006). Characterization of oligomers during α-synuclein aggregation using intrinsic tryptophan fluorescence. *Biochemistry*, **45**, 2752–2760.
14. Kaylor, J., Bodner, N., Edridge, S., Yamin, G., Hong, D. P. & Fink, A. L. (2005). Characterization of oligomeric intermediates in α-synuclein fibrillation: FRET studies of Y125W/Y133F/Y136F α-synuclein. *J. Mol. Biol.* **353**, 357–372.
15. Fernandez, C. O., Hoyer, W., Zweckstetter, M., Jares-Erijman, E. A., Subramaniam, V., Griesinger, C. & Jovin, T. M. (2004). NMR of α-synuclein-polyamine complexes elucidates the mechanism and kinetics of induced aggregation. *EMBO J.* **23**, 2039–2046.
16. Wu, C. W. & Yarbrough, L. R. (1976). N-(1-pyrene) maleimide: a fluorescent cross-linking reagent. *Biochemistry*, **15**, 2863–2868.
17. Karpovich, D. S. & Blanchard, G. J. (1995). Relating the polarity-dependent fluorescence response of pyrene to vibronic coupling. Achieving a fundamental understanding of the *py* polarity scale. *J. Phys. Chem.* **99**, 3951–3958.
18. Dong, D. C. & Winnik, M. A. (1984). The Py scale of solvent polarities. *Can. J. Chem.* **62**, 2560–2565.
19. Krishnan, R. & Lindquist, S. L. (2005). Structural insights into a yeast prion illuminate nucleation and strain diversity. *Nature*, **435**, 765–772.
20. Lin, T. I. (1982). Excimer fluorescence of pyrene-tropomyosin adducts. *Biophys. Chem.* **15**, 277–288.
21. Tcherkasskaya, O., Davidson, E. A., Schmerr, M. J. & Orser, C. S. (2005). Conformational biosensor for diagnosis of prion diseases. *Biotechnol. Lett.* **27**, 671–675.
22. Tamamizu-Kato, S., Kosaraju, M. G., Kato, H., Raussens, V., Ruysschaert, J. M. & Narayanaswami, V. (2006). Calcium-triggered membrane interaction of the α-synuclein acidic tail. *Biochemistry*, **45**, 10947–10956.
23. Wahl, P. (1979). Analysis of fluorescence anisotropy decays by a least square method. *Biophys. Chem.* **10**, 91–104.
24. Celej, M. S., Jares-Erijman, E. A. & Jovin, T. M. (2008). Fluorescent N-arylaminonaphthalene sulfonate probes for amyloid aggregation of α-synuclein. *Biophys. J.* doi:10.1529/biophysj.107.125211
25. Hammarstrom, P., Kalman, B., Jonsson, B. H. & Carlsson, U. (1997). Pyrene excimer fluorescence as a proximity probe for investigation of residual structure in the unfolded state of human carbonic anhydrase II. *FEBS Lett.* **420**, 63–68.

26. Winnik, F. M. (1993). Photophysics of preassociated pyrenes in aqueous polymer solutions and in other organized media. *Chem. Rev.* **93**, 587–614.
27. Piemonte, F., Caccuri, A. M., Morgenstern, R., Rosato, N. & Federici, G. (1993). Aggregation of pyrene-labeled microsomal glutathione *S*-transferase. Effect of concentration. *Eur. J. Biochem.* **217**, 661–663.
28. Heise, H., Hoyer, W., Becker, S., Andronesi, O. C., Riedel, D. & Baldus, M. (2005). Molecular-level secondary structure, polymorphism, and dynamics of full-length α-synuclein fibrils studied by solid-state NMR. *Proc. Natl Acad. Sci. USA*, **102**, 15871–15876.
29. Conway, K. A., Harper, J. D. & Lansbury, P. T., Jr. (2000). Fibrils formed in vitro from α-synuclein and two mutant forms linked to Parkinson's disease are typical amyloid. *Biochemistry*, **39**, 2552–2563.
30. Der-Sarkissian, A., Jao, C. C., Chen, J. & Langen, R. (2003). Structural organization of α-synuclein fibrils studied by site-directed spin labeling. *J. Biol. Chem.* **278**, 37530–37535.
31. Serpell, L. C., Berriman, J., Jakes, R., Goedert, M. & Crowther, R. A. (2000). Fiber diffraction of synthetic α-synuclein filaments shows amyloid-like cross-β conformation. *Proc. Natl Acad. Sci. USA*, **97**, 4897–4902.
32. Volles, M. J. & Lansbury, P. T., Jr (2007). Relationships between the sequence of α-synuclein and its membrane affinity, fibrillization propensity, and yeast toxicity. *J. Mol. Biol.* **366**, 1510–1522.
33. Lashuel, H. A., Petre, B. M., Wall, J., Simon, M., Nowak, R. J., Walz, T. & Lansbury, P. T., Jr (2002). α-synuclein, especially the Parkinson's disease-associated mutants, forms pore-like annular and tubular protofibrils. *J. Mol. Biol.* **322**, 1089–1102.
34. Uversky, V. N., Li, J. & Fink, A. L. (2001). Evidence for a partially folded intermediate in α-synuclein fibril formation. *J. Biol. Chem.* **276**, 10737–10744.
35. Michl, J. & Thulstrup, E. W. (1986). *Spectroscopy with Polarized Light–Solute Alignment by Photoselection, in Liquid Crystals, Polymers and Membranes,* p. 121, VCH, UK.
36. Uversky, V. N. (2003). A protein-chameleon: conformational plasticity of α-synuclein, a disordered protein involved in neurodegenerative disorders. *J. Biomol. Struct. Dynam.* **21**, 211–234.
37. Conway, K. A., Lee, S. J., Rochet, J. C., Ding, T. T., Williamson, R. E. & Lansbury, P. T., Jr (2000). Acceleration of oligomerization, not fibrillization, is a shared property of both α-synuclein mutations linked to early-onset Parkinson's disease: implications for pathogenesis and therapy. *Proc. Natl Acad. Sci. USA*, **97**, 571–576.
38. Allsop, D., Swanson, L., Moore, S., Davies, Y., York, A., El-Agnaf, O. M. & Soutar, I. (2001). Fluorescence anisotropy: a method for early detection of Alzheimer β-peptide (Aβ) aggregation. *Biochem. Biophys. Res. Commun.* **285**, 58–63.
39. Weltman, J. K., Szaro, R. P., Frackelton, A. R., Jr, Dowben, R. M., Bunting, J. R. & Cathou, B. E. (1973). N-(3-pyrene)maleimide: a long lifetime fluorescent sulfhydryl reagent. *J. Biol. Chem.* **248**, 3173–3177.
40. Foguel, D., Suarez, M. C., Ferrao-Gonzales, A. D., Porto, T. C., Palmieri, L., Einsiedler, C. M. *et al.* (2003). Dissociation of amyloid fibrils of α-synuclein and transthyretin by pressure reveals their reversible nature and the formation of water-excluded cavities. *Proc. Natl Acad. Sci. USA*, **100**, 9831–9836.
41. Ludescher, R. D., Peting, L., Hudson, S. & Hudson, B. (1987). Time-resolved fluorescence anisotropy for systems with lifetime and dynamic heterogeneity. *Biophys. Chem.* **28**, 59–75.
42. Luk, K. C., Hyde, E. G., Trojanowski, J. Q. & Lee, V. M. (2007). Sensitive fluorescence polarization technique for rapid screening of α-Synuclein oligomerization/fibrillization inhibitors. *Biochemistry*, **46**, 12522–12529.
43. Smith, W. S., Broadbridge, R., East, J. M. & Lee, A. G. (2002). Sarcolipin uncouples hydrolysis of ATP from accumulation of Ca^{2+} by the Ca^{2+}-ATPase of skeletal-muscle sarcoplasmic reticulum. *Biochem. J.* **361**, 277–286.